energies

MDPI

Article

Proposal for the Implementation of Solar Chimneys near Urban Environments with Variable Collector Area According to Demand and Environmental Conditions

Jorge Luis Mírez Tarrillo [1,†] and Jesús C. Hernandez [2,*,†]

[1] Group of Mathematical Modeling and Numerical Simulation (GMMNS), Faculty of Oil, Natural Gas and Petrochemical Engineering, National University of Engineering, Lima 5333, Peru; jmirez@uni.edu.pe
[2] Department of Electrical Engineering, University of Jaén, Campus Lagunillas s/n, Edificio A3, 23071 Jaén, Spain
* Correspondence: jcasa@ujaen.es
† These authors contributed equally to this work.

Abstract: This article reports the proposal for the use of towers solar (solar chimneys) in urban environments in order to take advantage of landfills, unpopulated or wild hills within or near cities, clearing landfills, artificial hills; considering that the solar tower can maintain the mechanical power of its wind turbine constant. To this end, a mathematical model has been developed to determine the collector area based on solar radiation and the mechanical power of the turbine. The present proposal has the potential that at a technical level there is the possibility of producing electrical energy, production of water intended to create/maintain green environments or for the population, hydrogen production, capture of atmospheric pollutants, measurement of air quality and elimination of cloud cover.

Keywords: solar chimmey; solar colector; smart cities; mountain; renewable energy sources; green energy; sustainable development; solar energy; power generation control

Citation: Tarrillo, J.L.M.; Hernandez, J.C. Proposal for the Implementation of Solar Chimneys near Urban Environments with Variable Collector Area According to Demand and Environmental Conditions. *Energies* **2024**, *17*, 5039. https://doi.org/10.3390/en17205039

Academic Editor: Francesco Nocera

Received: 12 September 2024
Revised: 30 September 2024
Accepted: 8 October 2024
Published: 10 October 2024

1. Introduction

The solar chimney power plant (SCPP) are a concept of harnessing solar radiation to generate electricity by creating an artificial greenhouse effect using a canvas or layer separated at a short distance from the ground. The electricity production is usually carried out by wind turbines. SCPPs usually consist of three components: a tower, a collector and one (or more) wind turbines. The collector converts the radiant energy of the Sun into thermal energy captured by the air between the collector membrane and the ground. This is an artificial greenhouse effect that leads to an increase in the temperature and speed of the air. A pressure difference is established due to the height of the tower, which causes the air to move from the outer contour of the collector to the lower part of the tower and then to be conducted to the upper part of the tower and evacuated to the outside atmosphere. Therefore, the design ensures a continuous flow of heated air with a performance regime based on the value of the environmental variables.

The first SCPP installation was installed in Manzanares, Spain (early 1980s) and there are several interesting works on it, which have been a source of ideas and concepts for the present paper. In [1] is reported that between July and September 1982, the maximum real power amounted to 41 kW for Manzanares SCPP and from their performance evaluation they mention that temporal variations in the driving factors of the plant, especially solar radiation, cause significant fluctuations in output power, therefore, they propose and evaluate dynamic and static control methods for attaining enhanced stability in power production within SCPP utilizing Fuzzy Logic Control (FLC) alongside Thermal Energy Storage (TES) systems. They develop a modeling of time-dependent performance for a

given value of collector area and the use of thermal energy storage in the collector floor. In [2] a innovative 3D axisymmetric computational fluid dynamics (CFD) is proposed and applied to Manzanares SCPP (Geometric specification: Average collector diameter = 244 m; chimney elevation = 194.6 m; chimney diameter = 10.6 m; average collector height = 1.85 m, and; ground thickness = 0.5 m); the variations in pressure, temperature, and speed profiles throughout the SCPP (from the collector inlet to the chimney outlet) are calculated using a computer with software in which a mathematical model of the physical system has been implemented the concerning fluctuations in solar radiation and ambient temperature, determining for example that for the solar radiation $G = 1000$ W/m^2), the maximum air speed V_m in the pilot plant is 14.24 m/s ($V_m = 4.92(1 - e^{-0.01883G} + 13.12(1 - e^{-0.001228G}))$), which aligns precisely with the experimental findings of 15.00 m/s; is observed that the stationary pressure P_s rapidly decline from the base of the chimney to the turbine entrance, afterward gradually increasing to the exhaust of the chimney; the lowest static pressure recorded is 100.18 Pa at a height of 21.92 m from the ground ($P_s = -114.7 + 106.1e^{-0.09357\psi} + 0.5924\psi$ where ψ is the position along the chimney); the SCPP's output power P_o increases linearly with the solar radiation ($P_o = -2879 + 50.21G$) whereas it steadily reduces with ambient temperature T_a ($P_o = 134600 - 291.9T_a$) and available power is equal to 49059 W for the case of 1000 W/m^2 and the atmospheric temperature of 293 K, and, mass flow rate ($\dot{m}$) of 1,118.85 kg/s with solar radiation of 1000 W/m^2 ($\dot{m} = 324.5 + 16150(1 - e^{-0.000022002G}) + 465.2(1 - e^{-0.003029G})$). In [3] a three-dimensional computational analysis to assess optimum collector inclination angle for the solar updraft tower power plant in Manzanares, which concludes that the collector inclination angle (θ) equal to 6° is its optimized inclination, because an angle of θ exceeding 7° caused air particles to circulate within the collector canopy, resulting in flow obstruction, whereas any angle of θ below 6° led to a decrease in key outputs such as theoretical power (Pth), collector efficiency (η_{coll}) and overall efficiency (η_o). In [4] using a three-dimensional model of the solar chimney on a 1:1 scale of the Manzanares SCPPS, Curved-Guide Vanes (CGVs), a blend of inlet guide vanes and central guides is introduced to assess the viability of utilizing CGVs in solar chimneys concerning efficiency. Five scenarios of 90°, 75°, 60°, 45°, and 30° CGVs were suggested, and the influence on the flow dynamics due to CGV angle has been analyzed initially within the chimney devoid of turbines. It was determined that the peak output power of 82.17 kW was achieved with 30° CGVs and 60 rpm. When compared to the output of the 90° CGVs, which served as the baseline scenario at the same rotational speed of 80 rpm, enhancements of 11.9% and 29.3% in output power were recorded for 60° and 30°, respectively. Concerning mass flow rate, for the case of the 90°, this exhibited the highest flow rate, approximately 752 kg/s at 20 rpm, however the 30° scenario displayed the lowest flow rate at around 532 kg/s at 100 rpm. The Manzanares prototype has led to further research such as: in [5] in which the study explores structural optimization aimed at mitigating the detrimental effects of environmental crosswinds on the efficiency of a solar chimney power plant system, examining scenarios with no baffle, a single baffle, and two baffles. The findings indicate that the average temperature at the chimney inlet with one baffle and two baffles is 0.92% and 3.92% greater than the scenario with no baffle, respectively; the average velocity at the chimney inlet with one baffle and two baffles is 11.83% and 18.70% higher than that of the no baffle case, respectively; and the average collector efficiency with one baffle and two baffles is 28.45% and 58.52% superior to that without any baffle, respectively; as well as mathematical study on solar chimney powerplant as in [6] where the influence of geometric factors like the angle of the collector roof (β), the divergent angle of the chimney (α), and wind speed on the efficiency of SCPP is examined, revealing that the power output of SCPP rises as β decreases at a constant α. To achieve peak performance from SCPP, the ratio of turbine pressure drop to overall pressure potential is set within the range of 0.7 to 0.85, and the increase in wind speed significantly boosts power production, and; and new collector designs such as in [7] in which is proposed and demonstrated that the dual-pass counter-flow collector

offers a highly effective approach that enhances the collector's performance by 28% when contrasted with the traditional collector.

The novel solar chimney concept involves the design and construction of a giant solar collector surrounding a hollow space excavated in a mountain in a region of stable geology has been proposed in [8]. They report that the hollow space can be used as an economical and safe updraft structural "chimney". but they only focus on the fact that it can be applied to mountains, they consider a fixed collector area and the mathematical model needs to be rewritten. That is why, in the present paper this concept can be applied to hills and mountains that can be found within or around cities, as well as in crop areas, landfills, recreational parks and/or around buildings where a shaded area is sought for a specific purpose.

In the case of crop areas, the collector is used to regulate the incident solar radiation on plants and/or create a protection zone against low temperatures during the night and/or winter. In landfills, the collector can be useful to maintain the temperature at an adequate value in order to maximize methane production or to maintain the temperature within a safe range that reduces the probability of spontaneous combustion of methane. In recreational parks and similar areas, the collector can be used to regulate the incident radiation on the public and to keep it within values that do not harm or damage health. Around buildings, the collector can take different forms and designs so that it can be part of vehicle parking lots, and among others; recreation, food and rest areas, air pollution mitigation (as in [9]), freshwater generation (as in [10]); inside buildings it can be used for cooling, as has been proposed by: ref. [11] that is a hybrid cooling-tower-solar-chimney system (HCTSC) that combining solar chimney and natural draft dry cooling tower; Ref. [12] where its implementation can aid in diminishing the power usage of conventional cooling systems, which is essential for data centers that are in growing number, size, complexity, and energy density resulting in considerable energy challenge; Ref. [13] where a new SCPP is reported and whose design consists in a collector connected to the building's wall (the building surfaces behave as energy absorbers) and is installed vertically on the roof of the building (which is different from conventional collectors such as Manzanares), but this proposal is studied on a small scale (solar chimney dimensions $175 \times 30 \times 80$ cm), while Manzanares has a mean collector radius = 122 m and few buildings in cities are more than 200 m long and 200 m high (approx. a building with 66 floors above street level); in [14] the capabilities of SCPP's technologies for building airflow, drinking water production, and electricity generation, in solitary, hybrid, and multi-use configurations have been thoroughly analyzed, emphasizing their ideal setup, advantages, disadvantages, and financial aspects. For instance, a solar chimney ventilation system composed of an earth-air heat exchanger and an evaporative cooler can reduce energy consumption for climate control activities by at least 20 to 75%. On the other hand, a standalone solar chimney power facility requires a significant land footprint and operates at an efficiency of just 1.0%. However, in hybrid and poly-generation scenarios, its efficiency has surged to 55%, and similarly in [15] which makes a review of design and performance analysis of solar chimney power plant (SCPP) and ref. [16] that offers an extensive overview of the last several decades and encompasses evaluations of the theoretical, experimental, and computational studies conducted to enhance the principal components of the system, such as the chimney, collector, and Power Conversion Unit (PCU), alongside other recently proposed innovative concepts and alternative technologies aimed at boosting SCPP efficacy. Meanwhile, other researchers directed their attention toward hybrid SCPPs to generate the desired by-product, like distilled water, thereby making SCPPs more viable; but in all the cases studied they have constant collector area.

Another viable implementation technique in the concept that we propose in this paper is the use of solar reflectors to redirect solar rays towards the collector in order to increase the temperature of the ground and the mass flow rate and enhance the efficiency and power output has been proposed by [17] and they reported that an increase of 9.89% in temperature of the floor and 134% in the mass flow rate, and, enhances 22.61% in the

efficiency and 133% in power output in comparation with a conventional SCPP without reflectors; in [18] with similar experiments with similar experiments, the results indicated a remarkable increase of up to 10.25% in the highest temperature measured at the base of the chimney, which led to a notable enhancement of 22.22% in the air flow speed. At the peak output, when power experienced a 56.867% boost compared to the daily average, the air flow speed showed a 25.316% rise, while the air density decreased by merely 2.069% from the average values for the day. Also, the integration of SCPP with photovoltaic solar panels as an in [19] in which the integration of photovoltaic panels with a slanted solar chimney is explored through an experimental framework (which includes a solar collector featuring a photovoltaic panel as the absorber, a chimney, and a convergent nozzle) alongside a numerical evaluation of the innovative hybrid system. The findings reveal that this hybrid configuration yields power efficiencies ranging from 9% to 11%, which is nearly two orders of magnitude superior to the conventional solar chimney efficiency. In addition, it demonstrates an enhancement of 18% when compared to the individual photovoltaic panel.

In summary, the state of the art shows as a fundamental characteristic, the realization of research from the point of view of a collector area of constant value, which once built cannot modify the area of the solar collector, and therefore, its operation becomes dependent on the incident solar radiation, which is random.

In [20] a collection of information on consumption habits, uses, equipment, and future demand projections of the Main Campus of the National University "Pedro Ruíz Gallo" in Lambayeque, Peru has been carried out. In addition, it is a delimited geographical area in whose surroundings there are schools, residential areas, markets, etc., where renewable energy sources such as solar energy and wind energy are locally available, with which it investigates and reports the improvement of energy efficiency through local production of renewable energy plants consisting of a 250 kWp photovoltaic solar plant and two 350 kW nominal capacity wind turbines. This place, due to its infrastructure and available renewable resources, is appropriate as a case study in this paper and, the average hourly solar radiation and ambient temperature data for the same period of time have been used (from 1 January 2018 to 28 March 2023).

Therefore, investigating the value of the collector area according to the solar radiation to maintain a fixed production of electric energy at a certain power, is important because it will allow the generation as a base type power plant that offers—in this case—a fixed electric power during some hours of the day. In the following part of this paper, the mathematical model and study scenario of electric demand and behavior of the variables involved according to different study scenarios will be studied. In the final part, a discussion of application perspectives in conjunction with other technologies reported in the scientific literature will broaden the vision of the application potential of this proposal.

2. Mathematical Model

The geometry to be considered is that of a truncated cone, which is an idealized shape of a mountain. The solar chimney concept consists of a solar collector which is implemented around the base of the mountain and the solar tower that goes in the central part of the mountain emulating the cone of a volcano. A duct dug into the mountain with a certain diameter and inclination connects the solar collector and the solar tower, and at the beginning of the duct, the wind turbine is placed (see Figure 1). The description is also applicable to the case of buildings since in the surroundings (vehicle parking, recreation and rest areas, exterior passageways, etc.) solar collectors can be arranged which channel the hot air towards the interior where one or more solar towers are arranged from the bottom to the top of the building (see Figures 1 and 2).

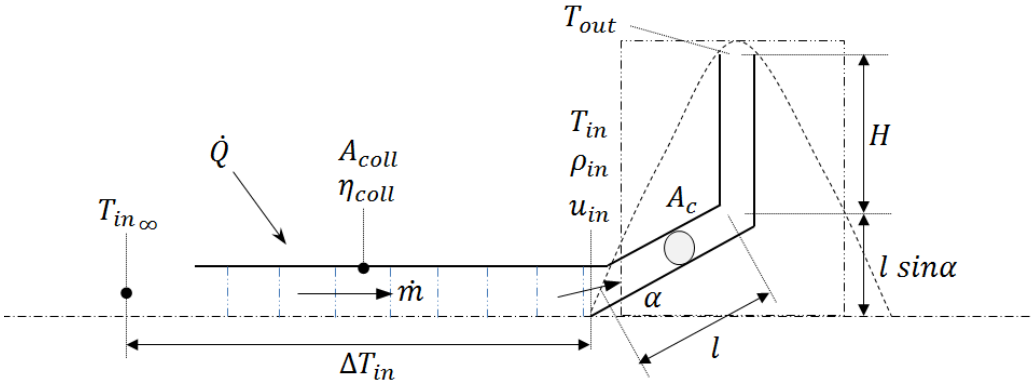

Figure 1. Proposal of integrating a solar collector with a man made mountain hollow (dotted curve in the form of a Gaussian function) or building (dotted rectangular curve representing a building with several levels or a certain height) following the idea reported in [8] where basically the collector area can be located in the available area at the foot of the mountain and regardless of the size of the area, the air flow can be channeled to the base of the chimney.

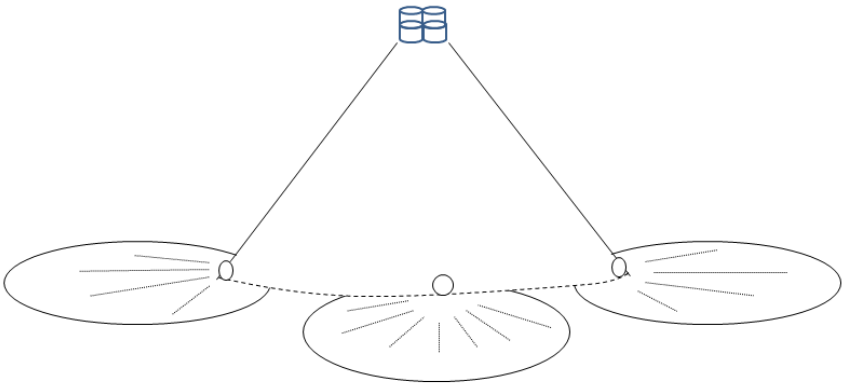

Figure 2. As a general concept is assumed that a mountain, a building or similar, on the reference surface, one or more solar collectors are installed, with each collector having its own solar tower that is placed inside the mountain (building or similar), which leads to having one or more outputs at the top. This design allows the characteristics of the environment around the mountain (building or similar) to be better used. Each solar collector heats and directs air to its respective wind turbine.

2.1. Mathematical Model of Chimney Solar of Low Height

The solar radiation G falls on the collector area A_{coll} which with some efficiency η_{coll} transmits that heat to the air below the solar collector, and the air has a heat capacity c_p. This heat transfer leads to an increase in air temperature $\triangle T_{in}$ and a mass flow rate of warm air flowing toward and through the mountain $\dot{m}$. The relationship between solar radiation, the solar collector and the moving air mass is shown in Equation (1) and the equivalence relations of $\triangle T_{in}$ is shown in the (2) and of $\dot{m}$ through the Equation (3) where T_{in} is the temperature of the air after passing through the solar collector, T_{in_∞} is the temperature of the air before entering the solar collector; ρ_{in} is the density of the air after passing through the solar collector, where A_c is the area of the duct that carries the air from the collector to the turbine and continues with the same area value in the solar tower; u_{in} is the wind speed at the end of its passage through the solar collector, and; Q is the heat captured by the air mass in transit below the solar collector.

$$GA_{coll}\eta_{coll} = \dot{Q} = c_p \dot{m} \triangle T_{in} \tag{1}$$

$$\triangle T_{in} = \frac{GA_{coll}\eta_{coll}}{c_p \dot{m}} = T_{in} - T_{in_\infty} \tag{2}$$

$$\dot{m} = \rho_{in} A_c u_{in} \tag{3}$$

The difference in pressure $\triangle P_c$ produced in the solar chimney can be determined by means of Equations (4) and (5), where H is the length of the solar tower (vertical) inside the mountain (or inside the building), l is the length of the connecting duct between the solar collector and the solar tower, α the angle of inclination of the connecting duct above the ground reference plane, ρ_{in_∞} is the density of the air before entering the solar collector, g is the Earth's gravity at the study site and ρ is the density of the air that changes as it moves through the solar tower.

$$\triangle P_c = g \int_0^{H+lsin\alpha} (\rho_{in_\infty} - \rho)\, dh \tag{4}$$

$$\triangle P_c = g \int_0^{H+lsin\alpha} \int_\rho^{\rho_{in_\infty}} d\rho\, dh \tag{5}$$

Then considering that $d\rho = -\beta\rho T$ where β is the coefficient of expansion of air and $\beta\rho$ remains constant—i.e. $(\beta\rho)_c$—throughout the entire route of the solar tower, that is, it can be written as $(\beta\rho)_c$; besides $\triangle P_c$ can be written according to Equation (6) and explicitly shows the relationship between the air temperature inside the solar tower and the height $T = T(h)$.

$$\triangle P_c = g(\beta\rho)_c \int_0^{H+lsin\alpha} (T - T_{in_\infty})\, dh \tag{6}$$

To solve Equation (6) is assumed that the temperature varies linearly with the height of the solar tower according to $T(h) = T_{in} + \gamma h - \alpha h$ where γ is the heat that enters from the mountain or building per unit of height measurement; α shows the variation of the air temperature in transit per meter of height of the solar tower and is defined as $\alpha = \frac{\triangle T_c}{H+lsin\alpha}$ and $\triangle T_c$ is the variation in air temperature between the air inlet and outlet of the solar tower and is expressed mathematically as $\triangle T_c = T_{in} - T_{out}$ where T_{out} is the temperature at which the air leaves the solar tower (upper hole of the solar tower); then, are obtained the Equations (7) and (8), and considering Equation (2) is obtained the Equation (9).

$$\triangle P_c = g(\beta\rho)_c \int_0^{H+lsin\alpha} \left[(T - T_{in_\infty}) + \left[\gamma - \frac{\triangle T_c}{H + lsin\alpha} \right] h \right] dh \tag{7}$$

$$\triangle P_c = g(\beta\rho)_c (H + lsin\alpha) \left[\triangle T_{in} + \frac{1}{2} [\gamma(H + lsin\alpha) - \triangle T_c] \right] \tag{8}$$

$$\triangle P_c = g(\beta\rho)_c (H + lsin\alpha) \left[\frac{G A_{coll} \eta_{coll}}{c_p \dot{m}} + \frac{1}{2} [\gamma(H + lsin\alpha) - \triangle T_c] \right] \tag{9}$$

The difference in pressure $\triangle P_c$ that occurs in the solar chimney can be represented as the set of pressure drops in each stretch (part, component) of the same as shown in Equation (10) where $\triangle P_f$ is the friction loss in the vertical and tilted chimney; $\triangle P_{in}$ is the chimney inlet loss; $\triangle P_l$ is the local resistence loss at the transition sections; $\triangle P_a$ is the vertical acceleration loss, and $\triangle P_{out}$ is the exit kinetic energy loss, parameters whose mathematical expression is shown in Equation (11) where ε_{in} is the chimney inlet loss coefficient; ε_l is the local resistance loss coefficient at the transition sections; f is the wall fricton factor; D is the diameter of A_c; ε_a is the vertical acceleration loss coefficient, and; ε_{out} is the exit kinetic energy loss coefficient.

$$\triangle P_c = \triangle P_{in} + \triangle P_l + \triangle P_t + \triangle P_f + \triangle P_a + \triangle P_{out} \tag{10}$$

$$\begin{aligned} \triangle P_{in} &= \varepsilon_{in}\frac{1}{2}\rho_{in}u_{in}^2 \\ \triangle P_{l} &= \varepsilon_{l}\frac{1}{2}\rho_{in}u_{in}^2 \\ \triangle P_{f} &= f\frac{H+l}{D}\rho_{in}u_{in}^2 \\ \triangle P_{a} &= \varepsilon_{a}\frac{1}{2}\rho_{in}u_{in}^2 \\ \triangle P_{out} &= \varepsilon_{out}\frac{1}{2}\rho_{in}u_{in}^2 \end{aligned} \tag{11}$$

The pressure drop due to the presence of the wind turbine $\triangle P_t$ is related to the mechanical power of the wind turbine W_t through the Equation (12) where A_c is the swept area of the turbine rotor (which coincides with the area of the duct that carries the air from the collector to the turbine) and u_{in} is the speed of the wind that hits the wind turbine (which coincides with the speed of the wind at the end of its passage through the solar collector). Therefore, using Equation (12) in Equation (10) is obtained the Equation (13).

$$\triangle P_t = \frac{W_t}{A_c u_{in}} \tag{12}$$

$$\triangle P_c = \triangle P_{in} + \triangle P_l + \triangle P_f + \triangle P_a + \triangle P_{out} + \frac{W_t}{A_c u_{in}} \tag{13}$$

So, the proposed operation of the solar chimney in this paper is that the pressure drop that occurs in the turbine $\triangle P_t$ is constant; and to achieve this, if is considered that η_{coll} has a constant value, G and $\dot{m}$ can vary, then it follows that the only way to regulate is by changing the value of the collector area A_{coll}.

The mathematical expressions of the electrical power generated by the wind turbine generator P_{out} and the overall efficiency of the solar chimney η are shown in Equations (14)–(16) where η_{t_g} is the efficiency of the wind turbine's electrical generator.

$$P_{out} = \eta_{t_g}\triangle P_t A_c u_{in} \tag{14}$$

$$\triangle P_t = \triangle P_c - \triangle P_{in} - \triangle P_l - \triangle P_f - \triangle P_a - \triangle P_{out} \tag{15}$$

$$\eta = \frac{P_{out}}{GA_{coll}} = \frac{\eta_{t_g}\triangle P_t A_c u_{in}}{GA_{coll}} \tag{16}$$

To determine the $\triangle T_c$ of the Equation (9), according to the theory of the law of conservation of mass in the chimney, is considered that $\rho_{in}u_{in} = \rho_{out}u_{out}$ and according to the First Law of Thermodynamics the equivalence between input and output energies of the solar chimney is shown in Equation (17) where e_{in} and e_{out} is the density of the air at the entrance and exit of the solar towers; p_{in} and p_{out} is the pressure at the entrance and exit of the solar tower; v_{in} and v_{out} is the volume per unit of mass at the entrance and exit of the solar tower; k_{in} and k_{out} is the kinetic energy of the air at the entrance and exit of the solar tower; gp_{in} and gp_{out} is the gravitational potential energy; q is the heat flow, and; W is the work.

$$e_{in} + p_{in}v_{in} + K_{in} + gp_{in} + q = e_{out} + p_{out}v_{out} + K_{out} + gp_{out} + W \tag{17}$$

For the ideal gas $e + pv = h_e = c_p T$ where he is the enthalpy and considering a certain mass flow $\dot{m}$ and turbine at the chimney inlet is obtained from Equations (18) and (19).

$$\begin{aligned} c_p\dot{m}(T_{in} - T_{out}) + \frac{1}{2}\dot{m}(u_{in}^2 - u_{out}^2) + \dot{m}g[0 - (H + lsin\alpha)] - \\ U(\overline{T} - \overline{T}_{m\infty})\pi D(H + lsin\alpha) = \triangle P_t A_c u_{in} \end{aligned} \tag{18}$$

$$\overline{T} = T_{in} - \frac{\triangle T_c}{2} \tag{19}$$

In addition, the total heat transfer coefficient between the air, the connecting duct and the mountain U is determined by Equation (20) where U_w describes the convective heat transfer coefficient between the chimney surface and the airflow within the solar chimney, and; U_{w_∞} denotes the heat transfer coefficient in the rocks of mountain.

$$U = \frac{1}{\left[\frac{1}{U_w} + \frac{1}{U_{w_\infty}}\right]} \tag{20}$$

Also, is determined $\triangle T_{in}$ through the Equation (21) which represents the increase in air temperature as it passes under the solar collector.

$$\triangle T_{in} = T_{in} - T_{in_\infty} \tag{21}$$

Then, from Equation (18) and considering Equation (12) is determined the Equations (22) and (23).

$$\begin{gathered} c_p \dot{m} \triangle T_c + \frac{1}{2}\dot{m}(u_{in}^2 - u_{out}^2) + \dot{m}g[-(H + lsin\alpha)] - \\ U(T_{in} - \frac{\triangle T_c}{2} - \overline{T}_{m\infty})\pi D(H + lsin\alpha) = \triangle P_t A_c u_{in} \end{gathered} \tag{22}$$

$$\begin{gathered} c_p \dot{m} \triangle T_c + \triangle T_c \frac{U\pi D(H + lsin\alpha)}{2} = \dot{m}g(H + lsin\alpha) + P_t A_c u_{in} - \\ \frac{1}{2}\dot{m}(u_{in}^2 - u_{out}^2) + U\pi D(H + lsin\alpha)(T_{in_\infty} + \triangle T_{in} - \overline{T}_{m\infty})) \end{gathered} \tag{23}$$

With this the total temperature difference across the solar chimney can be determined $\triangle T_c$ is shown in Equations (24) and (25).

$$\begin{gathered} \triangle T_c = \frac{\dot{m}g(H + lsin\alpha) + \triangle P_t A_c u_{in} - \frac{1}{2}\dot{m}\left[u_{in}^2 - u_{out}^2\right]}{\dot{m}C_p + \frac{U\pi D(H + lsin\alpha)}{2}} + \\ \frac{U\pi D(H + lsin\alpha)(T_{in_\infty} + \triangle T_{in} - T_{m_\infty})}{\dot{m}c_p + \frac{U\pi D(H + lsin\alpha)}{2}} \end{gathered} \tag{24}$$

$$\begin{gathered} \triangle T_c = \frac{\dot{m}g(H + lsin\alpha) - \frac{1}{2}\dot{m}\left[u_{in}^2 - u_{out}^2\right]}{\dot{m}c_p + \frac{U\pi D(H + lsin\alpha)}{2}} + \\ \frac{U\pi D(H + lsin\alpha)(T_{in_\infty} + \triangle T_{in} - T_{m_\infty}) + W_t}{\dot{m}C_p + \frac{U\pi D(H + lsin\alpha)}{2}} \end{gathered} \tag{25}$$

Finally, using Equation (9) and clearing, the solar collector area A_{coll} is expressed according to the Equation (26), which depends inversely of G and η_{coll} and directly from $\dot{m}$, $\triangle T_c$ and $\triangle P_c$.

$$A_{coll} = \frac{c_p \dot{m}}{G\eta_{coll}}\left[\frac{\triangle P_c}{g(\beta\rho)_c(H + lsin\alpha)} - \frac{1}{2}[\gamma_0(H + lsin\alpha) - \triangle T_c]\right] \tag{26}$$

2.2. Mathematical Model of Chimney Solar of High Height

For large height changes, considering Equation (27) is used the density ρ and ρ_{in_∞} according to Equations (28) and (29) where p is the local pressure and T is the air temperature in degrees Kelvin. The Equations (28) and (29) has been obtained from [21]. The local pressure p depends on the height z in meters above sea level, however, is possible to install both

temperature sensors T as local pressure p inside the solar chimney to obtain more adequate data or it can be determined experimentally using scale models.

$$\triangle P_c = g \int_0^{H+lsin\alpha} (\rho_{in_\infty} - \rho)\, dh \tag{27}$$

$$\rho = 3.4837 \frac{p}{T} \tag{28}$$

$$p = 101.29 - (0.011837)z + (4.793 \times 10^{-7})z^2 \tag{29}$$

In the Equation (29) z is expressed as $z = z_o + h$ where z_o is the height above sea level at which the ground level is located, on which the solar chimney is located, and, h is the height above ground level at which—depending on the height h—is located, the different parts of the solar chimney: collector, wind turbines, solar tower inlet, solar tower outlet. Therefore, ρ_{in_∞} is expressed according to Equation (30).

$$\rho_{in_\infty} = 3.4837 \frac{p_{z_o}}{T_{z_o}} \tag{30}$$

2.3. Mathematical Model of the Evolution of Air Temperature in the Collector

The air at ground level and around the solar chimney is driven towards the solar tower by the siphon effect created due to the difference in air density between ground level and around the outlet of the solar tower, therefore, the air is forced to pass under the cover of the solar collector where it receives heat and consequently, raises its temperature. In this subsection, a mathematical model is presented—using finite differences—of the evolution of the temperature that occurs in the air in its path under the cover of the solar collector.

Let an annular solar collector be located around a solar tower whose radius is r_o (see Figure 3). If is considered that the air advances from the outer contour of the solar collector with a certain constant speed, the location of a certain amount of air mass can be represented as an annular section, then, the solar collector can be discretized by calculating the areas of the annular section according to Equations (31)–(33).

$$A_R = \pi R^2 \tag{31}$$

$$A_r = \pi r^2 \tag{32}$$

$$\triangle A_a = \pi(R^2 - r^2) \tag{33}$$

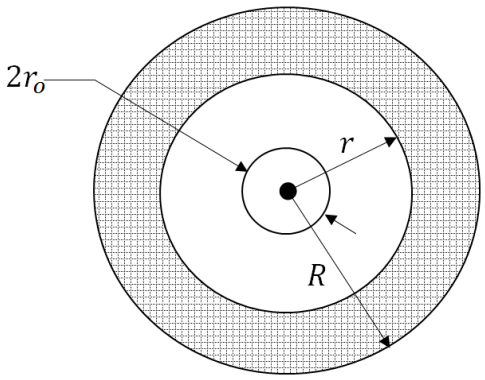

Figure 3. Annular discretization of a symmetrically shaped solar collector around a solar tower.

The heat incident on the collector area $\triangle Q$ is determined by Equation (34) where G is measured in W/m^2 and $\pi(R^2 - r^2)$ in m^2

$$\triangle Q = GA_a = G\pi(R^2 - r^2) \tag{34}$$

But this heat flow $\triangle Q$ occurs during a certain time on the canvas of the solar collector and the air that passes under the canvas, a mass of air that upon receiving this heat absorbs it according to Equation (35) and leads to a variation in temperature $\triangle T$.

$$\triangle Q = mc_p \triangle T \tag{35}$$

However, due to the symmetry with which the air travels under the solar collector's canvas, it can be assumed that there is a mass flow through radial current lines that for a certain air mass would create a radial section of a certain area from the outer contour to the inner contour of the solar collector, and that in its path the amount of heat received by the air mass can vary and therefore, the heat can be measured every second and/or every certain radial distance in the collector; a mechanism that is represented mathematically according to Equation (36).

$$\frac{\triangle Q}{\triangle t} = \frac{\triangle m}{\triangle t} c_p \triangle T \tag{36}$$

Let $\triangle t \mapsto 0$ then the instantaneous variation of solar radiation and mass flow is according to Equations (37)–(39).

$$\frac{dQ}{dt} = \frac{dm}{dt} c_p \triangle T \tag{37}$$

$$\dot{Q} = \dot{m} c_p \triangle T \tag{38}$$

$$G\pi(R^2 - r^2) = \dot{m} c_p \triangle T \tag{39}$$

But this increase in temperature will be carried out in steps, as the air travels through the collector, so the increase in temperature occurs progressively (see Figure 4), therefore, considering a mass flow $\dot{m}$, it has been established according the Equations (40) and (41).

$$G_i\pi(R_{t_i}^2 - r_{t_i}^2) = \dot{m} C p_{t_i} \triangle T \tag{40}$$

$$\triangle T = T_{t_{i+1}} - T_{t_i} \tag{41}$$

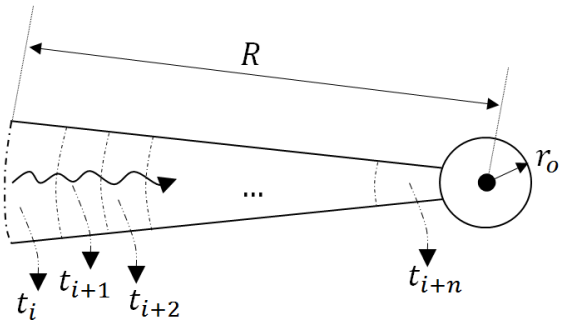

Figure 4. Discretization that represents the transit of a certain air mass through the solar collector from the outer edge to the boundary of the circumference of the solar tower where the wind turbines are located.

Then, according to Figure 5, certain mass m depends of the density ρ and volume V that occupies. The volume V will depend on the geometric characteristics of its radial path in the solar collector. (see Figure 5) and is expressed by Equation (42) where A is the perpendicular sectional area of the finite volume that occupies a certain mass to the direction of movement of the air in the solar collector, w is the width of the sectional area occupied by the mass m, h the height of the sectional area and l is the length of the sectional area occupied by a certain mass m.

$$m = \rho V = \rho A l = \rho w h l \tag{42}$$

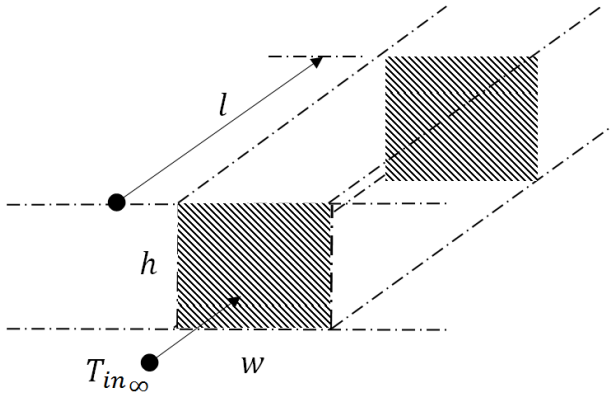

Figure 5. Representation of the finite volume occupied by a certain mass of air at a given moment in its path under the solar collector canvas.

Therefore, if is considered to mass flow $\dot{m}$ involves a renewal of the air mass that passes through a certain cross section of the solar collector and its advance is expressed as the speed v with which it moves under the solar collector canvas, expressed according to Equation (43).

$$\dot{m} = \rho A v = \rho w h v \tag{43}$$

So, the air mass passing through the solar collector can be expressed in a general way as a discrete motion of a certain mass flow $\dot{m}_i$ that instantly advances a distance l_i according to Equation (44) where $l'_i = \frac{dl_i}{dt}$.

$$\dot{m}_i = \rho_i w_i h_i \frac{dl_i}{dt} = \rho_i w_i h_i l'_i \tag{44}$$

Therefore, taking into consideration the discretization of the air movement in the collector, so, replacing Equation (44) in Equation (39) leads to Equation (45)

$$G_i \pi (r_{t_i}^2 - r_{t_{i+1}}^2) = \rho_{t_i} w_{t_i} h_{t_i} l'_{t_i} c_{p_{t_i}} \left[T_{t_{i+1}} - T_{t_i}\right] \tag{45}$$

but, in each unit of time (second), you have to $l'_{t_i} = r_{t_i} - r_{t_{i+1}}$, therefore, Equation (45) becomes Equations (46) and (47), of which by clearing is possible to determine the value of $T_{t_{i+1}}$ as shown in Equations (48) and (49).

$$G_i \pi (r_{t_i}^2 - r_{t_{i+1}}^2) = \rho_{t_i} w_{t_i} h_{t_i} \left[r_{t_i} - r_{t_{i+1}}\right] c_{p_{t_i}} \left[T_{t_{i+1}} - T_{t_i}\right] \tag{46}$$

$$G_i \pi (r_{t_i} + r_{t_{i+1}}) = \rho_{t_i} w_{t_i} h_{t_i} c_{p_{t_i}} \left[T_{t_{i+1}} - T_{t_i}\right] \tag{47}$$

$$T_{t_{i+1}} - T_{t_i} = \frac{G_i \pi (r_{t_i} + r_{t_{i+1}})}{\rho_{t_i} w_{t_i} h_{t_i} c_{p_{t_i}}} \tag{48}$$

$$T_{t_{i+1}} = T_{t_i} + \frac{G_i \pi (r_{t_i} + r_{t_{i+1}})}{\rho_{t_i} w_{t_i} h_{t_i} c_{p_{t_i}}} \tag{49}$$

Considering Equation (28), the Equation (49) becomes Equation (50), and if $r_{t_{i+1}} = r_{t_i} + \triangle r_{t_i \mapsto t_{i+1}}$ then is obtained the Equation (51).

$$T_{t_{i+1}} = T_{t_i} + \frac{I_i \pi (r_{t_i} + r_{t_{i+1}})}{\frac{3.4837p}{T_i + 273.15} w_{t_i} h_{t_i} c_{p_{t_i}}} \tag{50}$$

$$T_{t_{i+1}} = T_{t_i} + \frac{I_i \pi (2r_{t_i} + \triangle r_{t_i \mapsto t_{i+1}})}{\frac{3.4837p}{T_i + 273.15} w_{t_i} h_{t_i} c_{p_{t_i}}} \tag{51}$$

With this, several simulations can be made considering different study scenarios, varying: $\triangle r_{t_i \mapsto t_{i+1}}$, p, r_{t_i}, w_{t_i}, h_{t_i}, $c_{p_{t_i}}$.

It should be noted that with each increase in i, the air mass advances in its path through the collector, which has a finite size according to Equation (52) where r_o is the radius of the inner circle that contains the turbine or the edge (sectional area) of the turbine and/or entry into the adiabatic zone of ascent by the mountain of the air heated in the collector. Then the simulations would go by determining how the temperature T changes and what distance the air mass travels.

$$\sum_{i}^{n}\left[R - \triangle r_{t_i \mapsto t_{i+1}}\right] \geq r_o \tag{52}$$

The mathematical model made above must be adjusted in the event that the time between solar radiation measurements $t_{j+1} - t_j$ is much larger compared to the time between measurements of air velocities $t_{i+1} - t_i$ under the collector (see Figure 6), therefore, Equation (40) is rewritten as shown in Equations (53) and (54).

$$G_{t_j}\pi(R_{t_i}^2 - r_{t_i}^2) = \dot{m}c_{p_{t_i}}\triangle T \tag{53}$$

$$\triangle T = T_{t_{i+1}} - T_{t_i} \tag{54}$$

Has been considered G_{t_j} because the solar radiation values usually available are hourly average data such as those from NASA Power Access Viewer [22], however, the air movement under the solar collector canvas usually lasts a few seconds (wind speed under the collector), therefore, it is necessary to have an equivalent between reading times of solar radiation and position of a certain air mass in the solar collector, and which is shown in Equation (55)

$$t_{j+1} - t_j = \sum_{i=1}^{M} t_i \tag{55}$$

G_{t_j} can be quantified as W/(m^2 h) or take it to the scale of W/(m^2 s) and harmonize with the remaining equations that lead to quantifying the temperature of the air in its path under the collector.

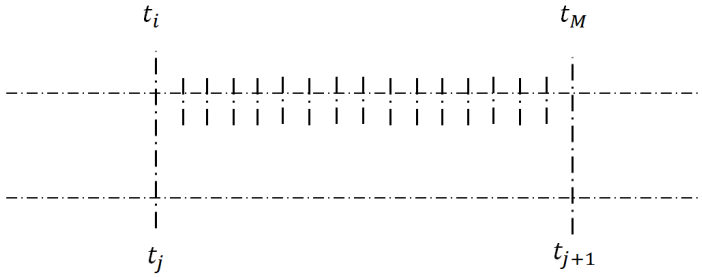

Figure 6. Diagram representing the equivalent in the discretization of solar radiation and wind speed reading times.

2.4. Data

The data has been obtained from NASA Power Access Viewer [22] and the location can be any one to choose, however, for the purposes of this research the University Campus of the National University "Pedro Ruíz Gallo" in the city of Lambayeque, Peru has been considered; with latitude −6.7077 and longitude −79.9075. The data collected is from 1 January 2018 to 28 March 2023; which is equivalent to 1912 days (5 years, 2 month and 27 days). During the study period, 14,560 h have been recorded in which solar radiation is ≥300 W/m^2, which results in 7.62 h per day with solar radiation ≥300 W/m^2. The Figure 7 shows the probability distribution of a certain value of solar radiation ≥300 W/m^2 during the daylight hours of the study period, and Figure 8 shows the probability distri-

bution of ambient temperature during the daylight hours of the study period with solar radiation $\geq$300 W/m^2.

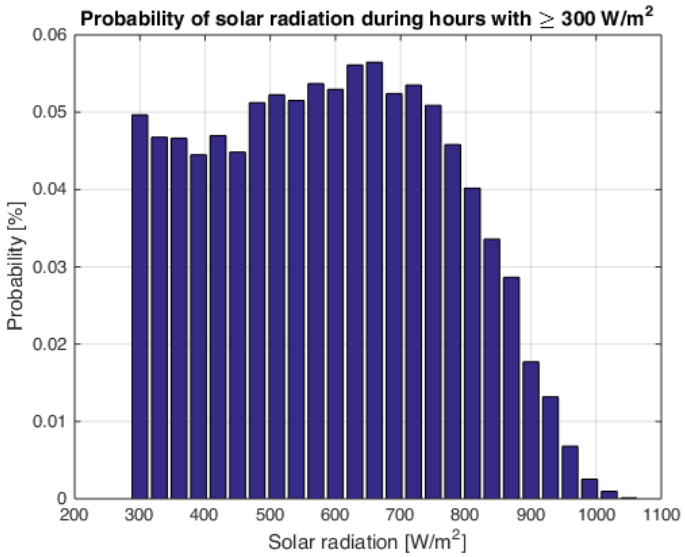

Figure 7. Probability of radiation solar during hours with $\geq$300 W/m^2 from 1 January 2018 to 28 March 2023.

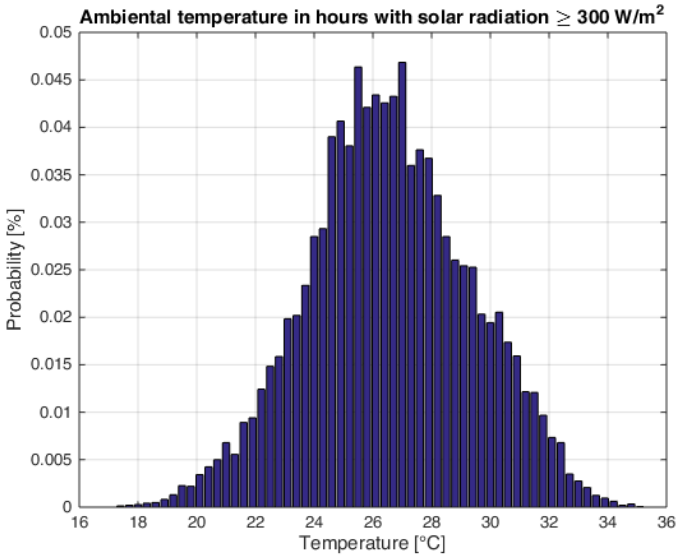

Figure 8. Probability of ambient temperature in hours with radiation solar $\geq$300 W/m^2 from 1 January 2018 to 28 March 2023.

3. Results

For the present paper, is used the constants described in Equation (56) obtained from [8] so that the pressures can be determined $\triangle P_{in}$, $\triangle P_l$, $\triangle P_f$, $\triangle P_a$ and $\triangle P_{out}$.

$$\begin{aligned} f &= 0.008428 \\ \varepsilon_{in} &= 0.056 \\ \alpha &= \pi/9; \\ \varepsilon_a &= 0.27 \\ \varepsilon_{out} &= 1.12 \\ \varepsilon_l &= 0.356 \end{aligned} \tag{56}$$

The Equation (26) leads to very large values in the early hours of the morning and during the late hours of the afternoon, this is because the value of G is reduced, and the A_{coll} must have a maximum size focused mainly on the hours of the day when solar radiation has been established at a value above a certain threshold (in addition, in all cases there will be a certain area available for the solar collector). The threshold for our case study is equal to or greater than 300 W/m^2.

Therefore, Table 1 and Figure 9 shows the hourly solar radiation data for the hours of interest on 1 January 2018 at the University Campus of the "Pedro Ruíz Gallo" National University, located in the city of Lambayeque, Peru; data that under the condition that T_{in_∞} is equal to 10 °C, are used to calculate the area of the solar collector that is necessary to have a mechanical power in wind turbine equal to 1 kW, whose value for each hour can be visualized in Figure 10 which shows that the necessary area must vary between approx. 2.5 ha to 5 ha, that is, approximately up to double its size compared to the area needed with the best solar radiation (711.08 W/m^2).

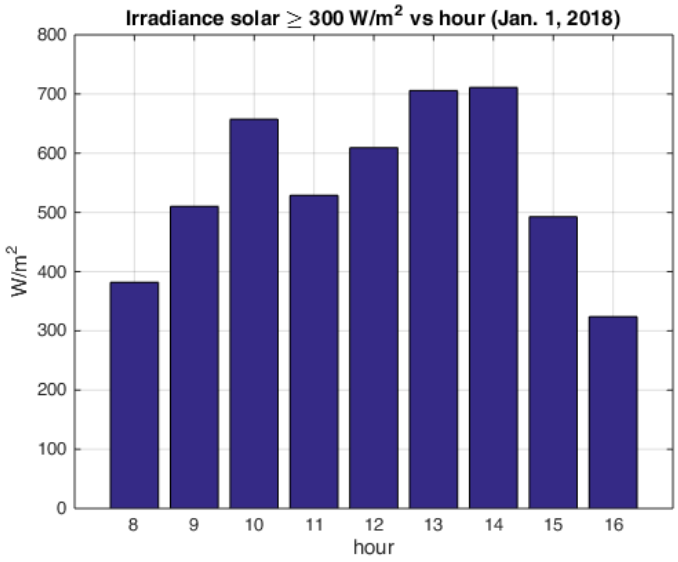

Figure 9. Evolution of solar radiation ≥300 W/m^2 during 1 January 2018.

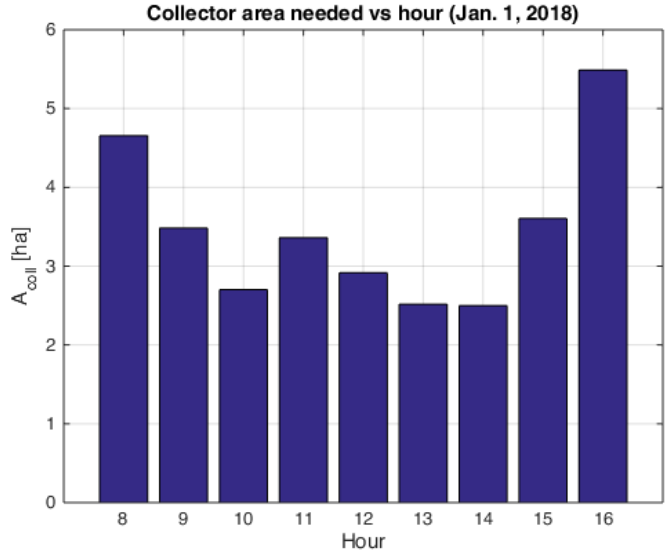

Figure 10. Evolution during hours of sunshine of the collector area needed to maintain constant mechanical power of the wind turbine.

Table 1. Data hourly of January 01, 2018 considered in simulation.

Hour	Hourly Solar Radiation
8:00	381.82
9:00	510.10
10:00	657.45
11:00	528.73
12:00	609.43
13:00	705.93
14:00	711.08
15:00	492.80
16:00	323.77 [1]

[1] Data may be shorter times between readings, but in this case has been used data obtained from NASA [22].

The Figure 11 shows the probability distribution of the collector area within the 5 ha considering all the hours of sunshine with solar radiation $\geq$300 W/m^2 that have been recorded during the study period.

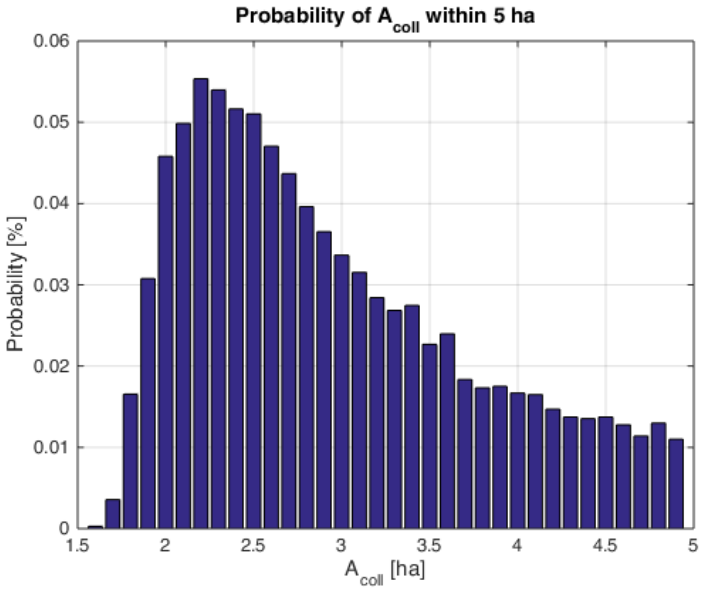

Figure 11. Probability of A_{coll} during hours with solar radiation $\geq$300 W/m^2 from 1 January 2018 to 28 March 2023.

4. Discussion

Has been frequently and usually considered in the design of solar chimneys, to have the solar collector with a defined and constant area, this implies that the electric power produced is based—mainly—on the incident solar radiation on the solar collector. Solar collector designs are usually circular around the solar tower, at least for the production of electric energy it has been considered this way, with an implementation in flat open spaces. In some cases, the solar collector is an annular section of fixed area for a specific purpose such as ventilation. Having a variable area collector implies for now, a challenge of mechanical and control design, which is natural due to the novel proposal made in this paper. However, in the short term, mechanical design accompanied by architectural design can create urban, semi-urban and rural spaces with multiple uses and benefits not only for people, but also for plants and animals. Among the uses and benefits that can be made and obtained from solar chimneys with variable collector area are:

- Generation of electric power and electrical storage for peak hours in order to reduce costs.
- It can also be used to keep the voltage stable.

- It can also be used to maintain the waveform, in this case, much depends on the type of storage used.
- The same energy that is produced can be used for filtering (purifying) the air.
- It allows the possibility of recording the composition of pollutants present in the air, which will greatly help to understand atmospheric dynamics.
- The volume of air that moves through the solar chimney during each hour and day can be quantified, and with this, determine the possibility of its use in air renewal in buildings or in urban spaces or in cities such as Lima (Peru) that have a cloud cover (fog, mist, smog) that remains fixed over the city for much of the year, or if there is the possibility of creating rain due to the rise of humid air to higher altitudes due to the siphon effect of the solar chimney.

5. Conclusions

The calculation demonstrates the technical possibility of maintaining a constant value of power produced by a solar chimney, which makes it a base power plant that delivers a constant power over a certain period of time. There is also the possibility of a third load, which can be, for example, hydrogen production and similar new technologies; these can make changes in the collector area but always under the premise of a constant power generation, so these third loads come to maintain constant demand. In addition, the increase/decrease of the solar collector area can be carried out through roller shutters that move on guides already installed. There is also the possibility that under the solar collector there are, for example, plants (and/or animals) that may well need direct sunlight for better growth (and/or breeding).

The proposal explained in this paper opens the possibility of developing calculation techniques for the sizing of variable area solar collectors using statistical techniques (mean value, standard deviation, histograms, etc.) and environmental variable data. An adequate area may involve not only the production of electric energy at a certain constant electric power, but other uses of the solar collector such as agriculture, feeding and raising small animals, recreation, thermal storage, heating, ventilation, among others. Based on the uses that will be given to it and building the mechanics necessary to vary the area of the collector; a design, installation and operating cost of the solar collector is defined, a subject that we leave for consideration for future research.

There is also the possibility of adaptation to demand, however, the recommendation is that this proposal for electricity generation always operates as a constant power plant.

Author Contributions: Conceptualization, J.L.M.T. and J.C.H.; methodology, J.L.M.T.; software, J.L.M.T.; validation, J.L.M.T. and J.C.H.; formal analysis, J.L.M.T. and J.C.H.; investigation, J.L.M.T. and J.C.H.; resources, J.L.M.T. and J.C.H.; data curation, J.L.M.T.; writing—original draft preparation, J.L.M.T.; writing—review and editing, J.L.M.T. and J.C.H.; visualization, J.L.M.T. and J.C.H.; supervision, J.C.H.; project administration, J.C.H.; funding acquisition, J.C.H. All authors have read and agreed to the published version of the manuscript.

Funding: This research received no external funding.

Data Availability Statement: The original contributions presented in the study are included in the article, further inquiries can be directed to the corresponding author.

Acknowledgments: The author acknowledge the support provided by the Thematic Network 723RT0150 "Red para la integración a gran escala de energías renovables en sistemas eléctricos (RIBIERSE-CYTED)" financed by the call for Thematic Networks of the CYTED (Ibero-American Program of Science and Technology for Development) for 2022.

Conflicts of Interest: The authors declare no conflicts of interest.

Abbreviations

The following abbreviations are used in this manuscript:

SCPP Solar chimney power plant

References

1. Tokfar, A.; Arefian, A.; Hosseini-Abardeh, R.; Bahrami, M. Implementation of active and pasive control strategies for power generation in a solar chimney power plant: A technical evaluation of Manzanares prototype. *Renew. Energy* **2023**, *216*, 118912. [CrossRef]
2. Cuce, E.; Cuce, P.M.; Sen, H. A thoroug performance assessment of solar chimney power plants: Case study for Manzanares. *Clean. Eng. Technol.* **2020**, *1*, 100026. [CrossRef]
3. Keshari, S.R.; Chandramohan, V.P.; Das, P. A 3D numerical study to evaluate optimum collector inclination angle of Manzanares solar updraft tower power plant. *Solar Energy* **2021**, *226*, 455-467. [CrossRef]
4. Xue, H.; Esmaeilpour, M. Power generation using solar energy: The effect of curved-guide vanes on the performance of a turbine in a solar chimney power plant. *Sol. Energy* **2022**, *247*, 468-484. [CrossRef]
5. Wang, J.; Nie, J.; Jia, J.; Su, H.; Tian, R.; Yan, S.; Gao, H. Structural optimization to reduce the environmental crosswind negative influence on the performance of a solar chimney power plant system. *Sol. Energy* **2022**, *241*, 693–711. [CrossRef]
6. Setareh, M. Comprehensive mathematical study on solar chimney powerplant. *Renew. Energy* **2021**, *175*, 470-485. [CrossRef]
7. Nasraoui, H. Novel collector design for enhancing the performance of solar chimney solar. *Renew. Energy* **2020**, *145*, 1658–1671. [CrossRef]
8. Zhou, X.; Yang, J.; Wang, J.; Xiao, B. Novel concept for producing energy integrating a solar collector with a man made mountain hollow. *Energy Convers. Manag.* **2009**, *50*, 847–854. [CrossRef]
9. Liu, Y.; Ming, T.; Peng, C.; Wu, Y.; Li, W.; de Richter, R.; Zhou, N. Mitigating air pollution strategies based on solar chimneys. *Sol. Energy* **2021**, *218*, 11–27. [CrossRef]
10. Wu, Y.; Ming, T.; de Richter, R.; Höffer, R.; Niemann, H.-J. Large-scale freshwater generation from the humid air using the modified solar chimney. *Renew. Energy* **2021**, *146*, 1325–1336. [CrossRef]
11. Zou, Z.; He, S. Modeling and characteristics analysis of hybrid cooling-towersolar- chimney system. *Energy Convers. Manag.* **2015**, *95*, 59–68. [CrossRef]
12. Guo, P.; Wang, S.; Lei, Y.; Li, J. Numerical simulation of solar chimney-based direct airside free cooling system for green data centers. *Energy Convers. Manag.* **2020**, *32*, 101793. [CrossRef]
13. Bagheri, S.; Hassanabad, M.G. Numerical and experimental investigation of a novel vertical solar chimney power plant for renewable energy production in urban areas. *Sustain. Cities Soc.* **2023**, *96*, 104700. [CrossRef]
14. Sharon, H. A detailed review on sole and hybrid solar chimney based sustainable ventilation, power generation, and potable water production systems. *Energy Nexus* **2023**, *10*, 100184. [CrossRef]
15. Pradhan, S.; Chakraborty, R.; Mandal, D.K.; Barman, A.; Bose, P. Design and performance analysis of solar chimney power plant (SCPP): A review. *Sustain. Energy Technol. Assess.* **2021**, *47*, 101411. [CrossRef]
16. Mehranfar, S.; Gharehghani, A.; Azizi, A.; Andwari, A.M.; Pesyridis, A.; Jouhara, H. Comparative assessment of innovative methods to improve solar chimney power plant efficiency. *Sustain. Energy Technol. Assess.* **2022**, *40*, 101807. [CrossRef]
17. Hussain, F.M.; Al-Sulaiman, F.A. Performance analysis of a solar chimney power plant design aided with reflectors. *Energy Convers. Manag.* **2018**, *117*, 30–42. [CrossRef]
18. Khidhir, D.K.; Atrooshi, S.A. Investigation of thermal concentration effect in a modified solar chimney. *Sol. Energy* **2020**, *206*, 799–815. [CrossRef]
19. Hussam, W.K.; Salem, H.J.; Redha, A.M.; Khlefat, A.M.; Al Khatib, F. Experimental and numerical investigation on a hybrid solar chimney-photovoltaic system for power generation in Kuwait. *Energy Convers. Manag. X* **2022**, *15*, 100249. [CrossRef]
20. Rubio, D.; Deciderio, E.Energy Management to Optimize Electrical Efficiency at the National University "Pedro Ruiz Gallo", Lambayeque, Peru . Ph.D. Thesis, National University "Pedro Ruiz Gallo", Lambayeque, Peru, 2023.
21. Manwell, J.F.; McGowan J.G.; Rogers, A.L. *Wind Energy Explained. Theory, Design and Application*, 2nd ed.; Wiley: West Sussex, UK, 2009; pp. 36–37.
22. NASA Prediction of Worldwide Energy Resources (POWER) | Data Access Viewer Enhanced (DAVe). Available online: https://power.larc.nasa.gov/data-access-viewer/ (accessed on 28 July 2024).